Selective uptake of organic dyes in a silver-based coordination polymer

Jia Zhang, Chong-Chen Wang, Peng Wang, Ya-Li Cao

Key Laboratory of Urban Stormwater System and Water Environment (Ministry of Education), Beijing University of Civil Engineering and Architecture, Beijing, 100044, China.

1 Experimental

1.1 Materials and methods

All chemicals and solvents were commercially available and used without any further purification. *Microcystis aeruginosa* was purchased from the Freshwater Algae Culture Collection of the Institute of Hydrobiology, Chinese Academy of Sciences (Wuhan, China). FTIR spectra in the region (400-4000 cm^{-1}), were recorded on a Nicolet 6700 FTIR spectrophotometer with KBr pellets. Powder X-ray diffraction (PXRD) patterns were recorded using a Dandonghaoyuan DX-2700B diffractometer with Cu Kα radiation. X-ray photoelectron spectra (XPS) measurement was demonstrated with Thermo ESCALAB 250XI. The elemental mapping was obtained on a Hitachi SU8020 scanning electron microscope (Tokyo, Japan). The microscope with Axio Imager A2 was used to observe the change of algae cells.

1.2 Synthesis of $[Ag_4(dpe)_4]\cdot(butca)\cdot 13H_2O$ (1)

An ammonia solution (125 mL, 0.5 mol/L) of $AgNO_3$ (1.25 mmol, 0.21 g) and 1,2,3,4-butanetetracarboxylic (H_4butca, 1.25 mmol, 0.29 g) was added dropwise to an EtOH solution (125 mL) of 1,2-di(4-pyridyl)ethylene (dpe, 1.25 mmol, 0.23 g), and the mixture was stirred for 15 min, then allowed to evaporate slowly at room temperature in the dark. Block-like white crystals of $[Ag_4(dpe)_4]\cdot(butca)\cdot 13H_2O$ (**1**) were obtained after 4 weeks (yield 90% based on $AgNO_3$). Anal. Calcd. for $C_{56}H_{72}Ag_4N_8O_{21}$ (%): C, 41.4; H, 4.4; N, 6.9. Found: C, 41.2; H, 4.3; N, 6.5. IR (KBr)/cm^{-1}: 3402, 1601, 1558, 1499, 1425, 1390, 1282, 1205, 1069, 1022, 1010, 998, 973, 871, 827, 548.

1.3 X-ray Single Crystal Analysis

The SMART software[1] was used for data collection of CP **1** and the SAINT software[2] for data extraction. Empirical absorption corrections were performed with the SADABS program[3]. The structures were solved by direct methods (SHELXS-97)[4] and refined by full-matrix-least squares techniques on F^2 with anisotropic thermal parameters for all of the non-hydrogen atoms (SHELXL-97)[4]. All hydrogen atoms were located by Fourier difference synthesis and geometrical analysis. These hydrogen atoms were allowed to ride on their respective parent atoms. All structural calculations were carried out using the SHELX-97 program package[4]. Crystallographic data and structural refinements for CP **1** are summarized in Table S1. Selected bond lengths and angles for CP **1** are listed in Table S2. The hydrogen bonds for CP **1** are illustrated in Table S3.

Table S1 Details of X-ray data collection and refinement for CP **1**

Formula	$C_{56}H_{72}Ag_4N_8O_{21}$	M (Mo,Kα) (mm^{-1})	1.219
M	1624.70	Total Reflections	33136
Crystal	Monoclinic	Unique	11853

Space group	$P2_1/n$	F (000)	3280
a, (Å)	15.6811(14)	Goodness-of-fit on F^2	1.075
b, (Å)	18.0103(15)	R_{int}	0.1027
c, (Å)	23.9667(19)	R_0	0.0699
α, (°)	90	$\omega R2$	0.1453
β, (°)	94.5940(10)	$R1$ (all data)	0.1960
γ, (°)	90	$\omega R2$ (all data)	0.1724
V, (Å^3)	6747.0(10)	Largest diff. peak and hole (e/Å^3)	1.332, -1.026
Z	4		

Table S2 Selected bond lengths (Å) and angles (°) for CP **1**

Bond lengths (Å)					
Ag(1)-N(1)	2.195(8)	Ag(1)-N(2)	2.220(8)	Ag(2)-N(4)	2.165(8)
Ag(2)-N(3)	2.201(8)	Ag(3)-N(6)	2.169(8)	Ag(3)-N(5)	2.188(8)
Ag(4)-N(7)	2.188(8)	Ag(4)-N(8)	2.208(8)		
Bond angles (°)					
N(1)-Ag(1)-N(2)	155.6(4)	N(4)-Ag(2)-N(3)	175.6(3)		
N(6)-Ag(3)-N(5)	174.2(4)	N(7)-Ag(4)-N(8)	155.5(4)		

Symmetry transformations used to generate equivalent atoms: #1 -*x*+1, -*y*+2, -*z*+1 #2 *x*+1/2, -*y*+3/2, *z*+1/2 #3 *x*-1/2, -*y*+3/2, *z*-1/2 #4 -*x*+2, -*y*+1, -*z*+1

Table S3 Hydrogen bonds for CP **1** [Å and °]

D-H	d(D-H)	d(H..A)	<DHA	d(D..A)	A
O9-H9C	0.850	2.006	168.01	2.842	O3
O9-H9D	0.850	2.332	166.87	3.165	O12 [x-1/2, -y+3/2, z-1/2]
O10-H10C	0.850	2.171	158.19	2.977	O6
O10-H10D	0.850	1.953	158.36	2.761	O7
O11-H11C	0.850	2.109	158.37	2.916	O1 [x, y-1, z]
O11-H11D	0.850	2.025	158.70	2.834	O3 [x, y-1, z]
O12-H12C	0.850	1.998	177.33	2.847	O6
O12-H12D	0.850	1.958	175.89	2.806	O13 [-x+1, -y+1, -z+1]
O13-H13C	0.850	1.953	174.96	2.801	O4 [-x+1/2, y-1/2, -z+1/2]
O13-H13D	0.850	1.953	174.99	2.801	O8 [x-1, y, z]
O14-H14C	0.850	1.993	175.47	2.841	O9
O14-H14D	0.850	2.075	176.61	2.924	O19 [-x+1, -y+2, -z+1]
O15-H15C	0.850	1.950	179.34	2.800	O1 [x, y-1, z]
O15-H15D	0.850	2.162	179.21	3.012	O17 [-x+1, -y+1, -z+1]
O16-H16C	0.850	2.086	177.98	2.936	O15 [-x+1, -y+1, -z+1]
O16-H16D	0.850	2.446	127.17	3.036	O16 [-x+2, -y+2, -z+1]
O17-H17C	0.850	1.934	166.25	2.767	O4
O17-H17D	0.850	2.514	168.13	3.351	O8 [-x+3/2, y+1/2, -z+1/2]
O18-H18C	0.850	1.964	173.22	2.810	O10 [-x+1, -y+1, -z+1]
O18-H18D	0.850	1.955	174.37	2.802	O18 [-x+1, -y+1, -z+1]
O19-H19C	0.850	1.979	172.48	2.824	O11 [-x+1, -y+1, -z+1]

O19-H19D	0.850	2.222	173.41	3.068	O16 [-x+2, -y+2, -z+1]
O20-H20C	0.850	2.122	135.71	2.794	O21'_b [-x+3/2, y+1/2, -z+1/2]
O20-H20C	0.850	2.419	140.08	3.119	O7
O20-H20D	0.850	2.213	133.97	2.869	O8
O20-H20D	0.850	2.607	132.74	3.244	O17 [-x+3/2, y-1/2, -z+1/2]
O21-H21E_a	0.850	2.057	178.93	2.907	O14 [x+1, y-1, z]
O21-H21F_a	0.850	2.142	176.50	2.991	O20 [-x+3/2, y-1/2, -z+1/2]
O21'-H21G_b	0.850	2.191	179.21	3.041	O7 [-x+3/2, y-1/2, -z+1/2]
O21'-H21H_b	0.850	1.523	179.52	2.373	O18 [x+1/2, -y+1/2, z-1/2]

Table S4 Defined ring and relative parameters of the π-π interactions in CP **1**

Cg(1): N(2)-->C(10)-->C(11)-->C(12)-->C(13)--> C(14)-->

Cg(2): N(7)-->C(45)-->C(46)-->C(47)-->C(48)-->C(49)-->

Cg(3): N(8)-->C(50)-->C(51)-->C(52)-->C(53)-->C(54)-->

Cg(4): N(3)-->C(17)-->C(18)-->C(19)-->C(20)-->C(21)-->

Cg(5): N(4)-->C(22)-->C(23)-->C(24)-->C(25)-->C(26)-->

Cg(6): N(5)-->C(33)-->C(34)-->C(35)-->C(36)-->C(37)-->

Cg(7): N(6)-->C(38)-->C(39)-->C(40)-->C(41)-->C(42)-->

Cg(8): N(1)-->C(5)-->C(6)-->C(7)-->C(8)-->C(9)-->

Cg(I) Cg(J)	Dist. Centroids (Å)	Dihedral angle(°)	Perp. Dist. (IJ) (Å)	Perp. Dist. (JI) (Å)
Cg(1)-->Cg(5)^{i*}	3.611(6)	6.1(5)	-3.429(4)	3.434(4)
Cg(2)-->Cg(6)^{i*}	3.644(6)	4.3(5)	-3.419(4)	3.502(4)
Cg(3)-->Cg(7)^{i*}	3.656(6)	4.5(5)	-3.500(4)	3.412(5)
Cg(4)-->Cg(8)^{i*}	3.665(6)	5.0(5)	-3.440(4)	3.538(4)

Symmetry codes: (i) *x*, *y*, *z*

1.4 Adsorption experiments

Methyl orange (MO), congo red (CR), methylene blue (MB) and rhodamine B (RhB) were selected as model pollutants to evaluate the adsorption performance of CP **1**. A solid sample (50 mg) of the CP **1** was added to 200 mL of MO (10 mg/L), CR (100 mg/L), MB (10 mg/L) or RhB (10 mg/L) aqueous solution in a 300 mL breaker. The mixtures were vibrated in water bath shaker with speed of 150 r/min at 293K. Sample of 1 mL aliquots were extracted using a 0.45μm syringe filter (Tianjin Jinteng) at regular intervals for analysis. A Laspec Alpha-1860 spectrometer was used to monitor the MO, CR, MB and RhB concentration changes by the maximum absorbance at 463, 493, 664 and 552 nm, respectively.

1.4.1 Adsorption kinetic

MO was selected as the removal target to study the kinetic adsorption process. Fifty micrograms CP **1** was added into 200 mL of MO (10, 20, 30 mg/L) solution at 293 K. All the mixtures were vibrated in constant temperature water bath shaker with speed of 150 r/min. One milliliter sample was drawn at a certain time interval with a 0.45 μm syringe filter, and analyzed by Laspec Alpha-1860 spectrometer.

Pseudo-first-order model[5] and the pseudo-second-order model[5] can be expressed as linear form by Equations (1) and (2):

$$\ln(q_e - q_t) = \ln(q_e) - k_1 t \quad (1)$$

$$\frac{t}{q_t} = \frac{1}{k_2 q_e^2} + \frac{1}{q_e} t \quad (2)$$

where q_t (mg/g) and q_e (mg/g) represent the amount of adsorbates adsorbed onto absorbents at t and at equilibrium time, respectively. k_1 (min^{-1}) represents the adsorption rate constant which is calculated from the plot of $\ln(q_e - q_t)$ against t. k_2 (g/(mg·min)) is the pseudo-second-order rate constant of sorption. The plot of t/q_t vs. t is expected to exhibit a linear relationship, and the q_e and k_2 can be obtained from the slope and intercept of the plot, respectively.

Table S5 Parameters of kinetic model of MO adsorption onto CP **1**

			Pseudo-first-order			Pseudo-second-order		
C_0 (mg/L)	CP **1** (mg)	$q_{e,exp}$ (mg/g)	k_1(min^{-1})	$q_{e,cal}$ (mg/g)	R^2	k_2 (g/(mg·min))	$q_{e,cal}$ (mg/g)	R^2
10		39.67	0.080	26.71	0.968	0.0044	42.61	0.997
20	50	79.07	0.074	90.01	0.992	0.0004	103.09	0.951
30		118.97	0.051	133.81	0.987	0.0002	159.74	0.993

1.4.2 Adsorption isotherms

In addition, the batch adsorption was adopted to measure the adsorption isotherms and mechanism of the adsorbent for the organic dye MO. 50 mg of CP **1** was placed into 200 mL MO aqueous solution with initial concentrations of 60, 90, 120, 150, 180 mg/L. The mixtures were vibrated in constant temperature water bath shaker with speed of 150 r/min at different temperatures like 288, 293, 298, 303 and 308 K, respectively. When adsorption equilibrium was reached, the suspensions were filtered through 0.45 μm syringe filter to analyze the changes of the MO concentration.

In this study, three isotherm models including Langmuir, Freundlich, and Dubinin–Radushevich (D-R) were utilized to describe equilibrium adsorption data.

The Langmuir isotherm model is listed in Equation (3)[6].

$$C_e / q_e = 1/(K_L q_{\max}) + C_e / q_{\max} \quad (3)$$

Where, q_{max} is the maximum adsorption capacity (mg/g) of adsorbent. K_L is related to the energy of adsorption which indicates the intensity of adsorption (L/mg); high K_L values mean strong bonding between the adsorbate and adsorbent.

The validity of the Freundlich isotherm model is proved by using Equation (4)[7]:

$$\log q_e = \log K_f + (1/\mathrm{n}) \log \mathrm{C}_e \quad (4)$$

Where K_f (mg/g) is the measure of adsorption capacity, $1/n$ is adsorption intensity. A plot of $\log q_e$ against $\log C_e$ gives a straight line, the slope and intercept of which correspond to $1/n$ and $\log K_f$, respectively. High K_f values indicate easy uptake of the adsorbate. The slope $1/n$ of Freundlich equation indicates the surface heterogeneity of the adsorbent, where $1/n$ values of closer to zero is indicative of relative energy distribution on the adsorbent surface (or surface heterogeneity).

The D-R isotherm can be described as Equation (5)[8]:

$$\ln q_e = \ln q_m - K_{DR} \varepsilon^2 \quad (5)$$

Where, K_{DR} is a constant related to the mean free energy of adsorption (mol^2/J^2), q_m is the theoretical saturation capacity (mol/g), ε is the potential (J/mol), which is related to equilibrium concentration C_e

(mg/L) as Equation (6):

$$\varepsilon = RT\ln(1+1/C_e) \quad (6)$$

The slope of the plot of ln q_e vs ε^2 gives K_{DR} and intercept yields the adsorption capacity q_m. The mean free energy of adsorption (E, kJ/mol) is calculated from Equation (7)

$$E = \frac{1}{\sqrt{2K_{DR}}} \quad (7)$$

Table S6 Constants of Langmuir, Freundlich, and D–R for MO adsorption by CP **1** at different temperatures

T/K	Langmuir			Freundlich			D-R		
	q_{max} (mg/g)	K_L (L/mg)	R^2	K_f (L/g)	*1/n*	R^2	K_{DR}	*E* (kJ/mol)	R^2
288	435	3648	0.985	30.74	0.490	0.997	0.00007	0.085	0.863
293	455	5844	0.978	48.68	0.428	0.993	0.00003	0.129	0.803
298	500	7541	0.987	51.27	0.440	0.989	0.00003	0.129	0.838
303	556	10193	0.987	52.81	0.472	0.974	0.00003	0.129	0.881
308	625	27174	0.983	52.96	0.488	0.992	0.00002	0.158	0.832

1.4.3 Thermodynamic parameters

Standard free energy (ΔG^0, kJ/mol), change in enthalpy (ΔH^0, kJ/mol) and change in entropy (ΔS^0, J/(mol·K)), were calculated with the help of data obtained from Langmuir adsorption isotherm via Equations (8) and (9).

$$\Delta G^0 = -RT\ln K_L \quad (8)$$

$$\ln K_L = \frac{\Delta S^0}{R} - \frac{\Delta H^0}{RT} \quad (9)$$

Where R is the ideal gas constant [8.314 kJ/ (mol·K)], T is the absolute temperature (K), K_L is the distribution coefficient at different temperatures. From Equation 8, ΔG^0 could be figured out, and the values of ΔS^0 and ΔH^0 can be obtained from the slope and the intercept of the linear plot of lnK_L *vs.* 1/T, respectively.

Table S7 Thermodynamic parameters for sorption process of MO on CP **1** at different temperatures

T/K	K_L (L/mg)	ΔG^0 (kJ/mol)	ΔS^0 (J/mol/K)	ΔH^0 (kJ/mol)
288	3648	-50.96		
293	5844	-52.99		
298	7541	-54.53	410	67.17
303	10193	-56.20		
308	27174	-59.64		

1.5 Regeneration experiment

About 50 mg of CP **1** as an adsorbent was added into 200 mL MO (10 mg/L) with constant vibration. After completion of each cycle (60 min), the adsorbent was collected through filtered and washed repeatedly with ethanol to remove any residual adsorbing solution. The adsorbent after drying was placed into MO (10 mg/L) solution for the second to fifth consecutive cycles. There are overall five

cycles, and the removal rates of MO were calculated based on the absorbance 464 nm in each cycle.

1.6 Antibacterial activity test

The CP **1** was using to conduct antibacterial experiment by the diffusion method described by Fiebelkorn et al.[9] Agar plate diffusion assay was the standardized method suggested by the National Committee for Clinical Laboratory Standards, based on the method described by Bauer et al.[10] Surface layer of lake water was used to investigate the antibacterial properties of CP **1**. Fifty micrograms of CP **1** was added to 50 mL lake water, and the control experiment was conducted at the same time without CP **1**. After 4 h cultivation, the supernatant was vaccinated onto Agar plate to observe the growth status of bacterial colony. The number of bacterial colony was 13400/mL (in the absence of CP **1**) and 153/mL (in the presence of CP **1**), as shown in the Fig. S1. The results demonstrated that CP **1** exhibited remarkable antibacterial properties.

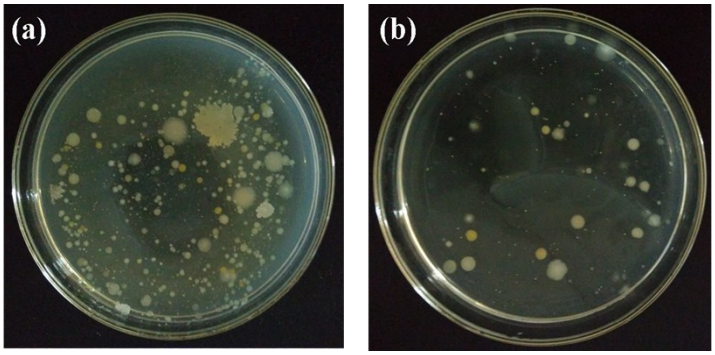

Fig. S1 Agar plate diffusion experiment to estimate antibacterial activity of CP 1 onto surface layer of lake water ((**a**) in the absence of CP **1**, (**b**) in the presence of CP **1**. Incubation conditions, 310 K, 24 h)

1.7 Antialgal activity test

In order to investigate the antialgal properties of CP **1**, *Microcystis aeruginosa* was selected as target to conduct experiment. A solid sample (50 mg) of CP **1** was placed into the *Microcystis aeruginosa* solution (50 mL 1.04×10^8 cells/mL). After 6 h cultivation, the algae cell density increased to 1.42×10^8 cells/mL (in the absence of CP **1**) and decreased to 1.82×10^3 cells/mL (in the presence of CP **1**), as shown in the Fig. S2. The results demonstrated that CP **1** could efficiently inhibit the growth of algae cells and kill the algae cells.

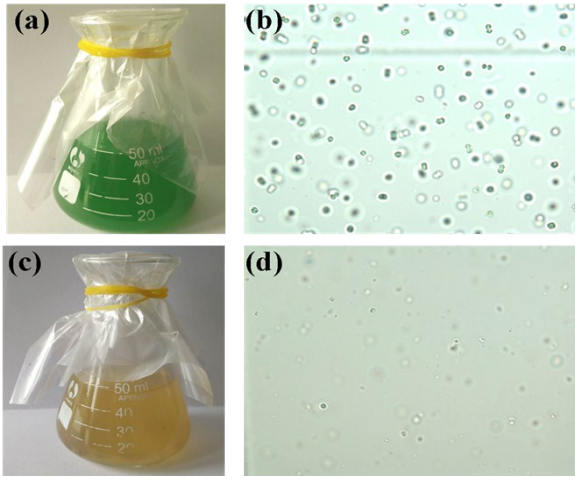

Fig. S2 The picture of *Microcystis aeruginosa* solution (**a**) and the algae cells under microscope (**b**) (in the absence of CP **1** after 6 h). The picture of *Microcystis aeruginosa* solution (**c**) and the algae cells under microscope (**d**) (in the presence of CP **1** after 6 h).

1.8 Separation experiment

In the separation study, dyes mixture solution with the initial concentration of MO (10 mg/L) and MB (10 mg/L) was prepared. The amount (50 mg) of CP **1** was added to a breaker containing 200 mL of mixture dye solution. Samples of different adsorption time were extracted and analyzed with Laspec Alpha-1860 spectrometer to confirm the concentration of MO and MB retaining in the solution.

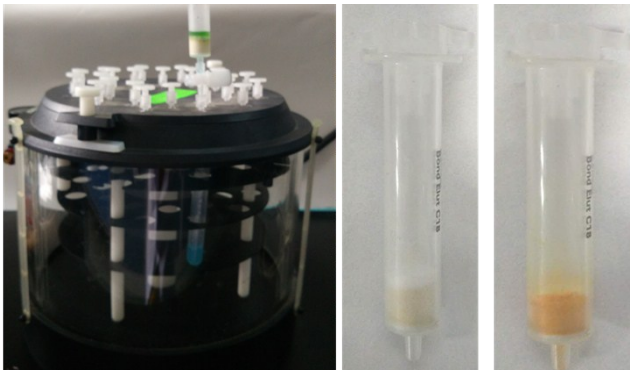

Fig. S3 The picture of SPE setup, in which the original packing material C18 was replaced by CP **1**

References

1. Bruker AXS SMART, Version 5.611, Bruker AXS, Madison, WI, USA, 2000.
2. Bruker AXS SAINT, Version 6.28, Bruker AXS, Madison, WI, USA, 2003.
3. SADABS V2.03, Bruker AXS, Madison, WI, 2000.
4. G. M.Sheldrick SHELX-97, Göttingen University, Germany, 1997.
5. Y.-S. Ho, *J. Hazard. Mater.*, 2006, 136, 681-689.
6. I. Langmuir, *J. Am. Chem. Soc.*, 1916, 38, 2221-2295.
7. H. Freundlich, *J. Phys. Chem*, 1906, 57, e470.
8. M. Dubinin and L. Radushkevich, *Doklady Akademii Nauk SSSR, Ser. Khim*, 1947, 55, 331.
9. K. Fiebelkorn, S. Crawford, M. McElmeel and J. Jorgensen, *J. Clin. Microbiol.*, 2003, 41, 4740-4744.
10. A. Bauer, W. Kirby, J. C. Sherris and M. Turck, *Am. J. Clin. Pathol.*, 1966, 45, 493.